Published in final edited form as:
Chembiochem. 2010 May 17; 11(8): 1093–1106. doi:10.1002/cbic.200900671.

Sesquiterpene synthases Cop4 and Cop6 from *Coprinus cinereus*: Catalytic promiscuity and cyclization of farnesyl pyrophosphate geometrical isomers

Fernando Lopez-Gallego[a], **Sean A. Agger**[a], **Daniel A. Pella**[b], **Mark D. Distefano**[b], and **Claudia Schmidt-Dannert**[a],*

[a] Department of Biochemistry, Molecular Biology and Biophysics, University of Minnesota, 1479 Gortner Avenue, St. Paul, MN 55108

[b] Department of Chemistry, University of Minnesota, 207 Pleasant Street SE, Minneapolis, MN 55455

Abstract

Sesquiterpene synthases catalyze with different catalytic fidelity the cyclization of farnesyl pyrophosphate (FPP) into hundreds of known compounds with diverse structures and stereochemistries. Two sesquiterpene synthases, Cop4 and Cop6, were previously isolated from *Coprinus cinereus* as part of a fungal genome survey. This study investigates the reaction mechanism and catalytic fidelity of the two enzymes. Cyclization of all-trans-FPP ((*E*,*E*)-FPP) was compared to the cyclization of the cis-trans isomer of FPP ((*Z*,*E*)-FPP) as a surrogate for the secondary cisoid neryl cation intermediate generated by sesquiterpene synthases capable of isomerizing the C2-C3 π bond of *all-trans*-FPP. Cop6 is a "high-fidelity" α-cuprenene synthase that retains its fidelity under various conditions tested. Cop4 is a catalytically promiscuous enzyme that cyclizes (*E*,*E*)-FPP into multiple products, including (−)-germacrene D and cubebol. Changing the pH of the reaction drastically alters the fidelity of Cop4 and makes it a highly selective enzyme. Cyclization of (*Z*,*E*)-FPP by Cop4 and Cop6 yields products that are very different from those obtained with (*E*,*E*)-FPP. Conversion of (E,E)-FPP proceeds via a *(6R)*-β-bisabolyl carbocation in the case of Cop6 and an (*E*,*E*)-germacradienyl carbocation in the case of Cop4. However, (*Z*,*E*)-FPP is cyclized via a (*6S*)-β-bisabolene carbocation by both enzymes. Structural modeling suggests that differences in the active site and the loop that covers the active site of the two enzymes may explain their different catalytic fidelities.

Keywords

Sesquiterpene synthase; farnesyl pyrophosphate; catalytic promiscuity; fungal; *Coprinus cinereus*

Introduction

Promiscuity of function is increasingly recognized as a property of many enzymes important for understanding enzyme evolution and function and for the engineering of better enzymatic catalysts for a variety of applications [1,2]. A group of enzymes especially known for their catalytic promiscuity are the terpene synthases and in particular, the sesquiterpene synthases.

*Address correspondence to: Dr. Claudia Schmidt-Dannert, Department of Biochemistry, Molecular Biology and Biophysics, University of Minnesota, 1479 Gortner Avenue, St. Paul, MN 55108, Tel. 612 625-5782; Fax. 612 625-5780; schmi232@umn.edu.

Supporting information for this article is available on the WWW under http://www.chembiochem.org or from the author.

This group of terpene synthases catalyzes the cyclization of the linear 15-carbon isoprene pyrophosphate substrate all-trans farnesyl diphosphate (*(E,E)*-FPP[1]) into more than 300 known mono-, bi- or tricyclic hydrocarbon or alcohol compounds with diverse stereochemistries [3]. The resulting terpenoid hydrocarbons are intermediates in the biosynthesis of biologically active compounds that are produced by plants, bacteria and fungi as antibiotics, toxins and pheromones [4,5]. Sesquiterpene synthases catalyze some of the most complex carbon-carbon bond forming reactions found in chemistry and biology [6]. Several mutagenesis and protein engineering studies aimed at understanding terpene cyclization [3] and modified product profiles of terpene synthases [7–9] have been published.

Cyclization of *(E,E)*-FPP is initiated by pyrophosphate cleavage, generating an initial substrate carbocation which is rearranged and eventually quenched by a water molecule or by proton abstraction from the substrate. The active site of the enzyme functions as a chaperone that folds the isoprenoid chain, shields the carbocation from premature nucleophilic attack and guides carbocation rearrangement until its final quenching [10]. The conformation of the bound isoprenyl chain and the residues lining the active site binding pocket determine carbocation reactions and hence, the final product profile of a particular sesquiterpene synthase.

Two consensus sequences - an aspartate rich DDXXD/E and a NSE/DTE motif - located at the entrance of the active site coordinate a trinuclear Mg^{2+} cluster that ligands the diphosphate moiety of the isoprenoid substrate, positions the isoprenyl chain in the binding pocket and triggers closure of the active site along with diphosphate cleavage to generate an initial transoid, allylic carbocation [11–13]. Enzymes that catalyze the trans-pathway of catalysis rearrange and quench this initial transoid cation. Other enzymes that catalyze the cis-trans pathway of catalysis recapture the diphosphate leaving group at carbon C3, thereby allowing rotation around the generated C2-C3 single bond to yield the nerolidyl diphosphate (NPP) intermediate. Depending on the binding of FPP in the active site, the configuration at C3 of the NPP intermediate can be *R* or *S*. This intermediate yields upon secondary diphosphate cleavage a cisoid, allylic cation that is subsequently rearranged and eventually quenched [14,15].

Sesquiterpene synthases are known that are very specific for either one or the other pathway of catalysis, while yet other enzymes utilize both pathways. Examples of trans-pathway specific enzymes with solved crystal structures include pentalenene synthase form *Streptomyces* UC5319 [16], 5-epi-aristolochene synthase from *Nicotiana tobaccum* [17,18] and aristolochene synthases from *Aspergillus terreus* and *Penicillium roqueforti* [19,20]. Trichodiene synthase from *F. sporotrichoides* [21,22] and very recently, δ-cadinene synthase from *Gossypium arboreum* (cotton) [23] are the only cis-trans pathway specific sesquiterpene synthase with a solved crystal structure. Examples for catalytically very promiscuous sesquiterpene synthases are γ-humulene synthase and δ-selinene synthase from *grand fir*. Each enzyme produces more than 30 sesquiterpene structures (cis-trans and trans-pathway products) in addition to their major products γ-humulene (cis-trans-pathway product) and δ-selinene (trans-pathway product) [15].

Previously, we have isolated two new cis-trans-pathway specific sesquiterpene synthases, Cop4 and Cop6, from the homobasidiomycete *Coprinus cinereus* as part of a survey of sesquiterpene synthase homologs present in fungal genomes [24,25]. Although both enzymes catalyze the isomerization of the C2-C3 bond of the farnesyl substrate, subsequent cyclization reaction differ greatly between the two enzymes as do their catalytic promiscuities. Cop 4 produced several volatile sesquiterpene products, including δ-cadinene as the major product, when expressed in *E. coli*. In contrast, Cop6 expressed in *E. coli* produced selectively α-

[1]The abbreviations used are: FPP, farnesyl diphosphate (also – pyrophosphate); NPP, nerolidyl diphosphate; GPP, geranyl diphosphate; PPi, pyrophosphate.

cuprenene, which is the precursor of the lagopodin antibiotics reported to be produced by *Coprinus* species[26].

In this work we performed kinetic and mechanistic studies with purified enzymes to investigate the different promiscuous behaviors of the two enzymes. We demonstrate that while Cop4, unlike Cop6, exhibits a very broad product profile with *(E,E)*-FPP under typical reaction conditions, the catalytic fidelity of Cop4 can be drastically altered by varying reactions conditions. Structural modeling of Cop4 and Cop6 suggests reasons for the differences in catalytic fidelity observed for the two enzymes.

In addition to analyzing the cyclization routes of *(E,E)*-FPP catalyzed by the two Cop enzymes, we use the cis-trans isomer of FPP (*(Z,E)*-PP) as a surrogate for the secondary cisoid neryl cation intermediate generated by sesquiterpene synthases that can isomerize the C2-C3 π bond of *all-trans*-FPP. Here, we ask the question whether the cyclization of the cis-isomer of FPP (*(Z,E)*-FPP) where the C2-C3 π bond is already in the cis-configuration would yield with Cop4 and Cop6 the same product profiles and promiscuous behaviors as observed with their normal substrate *(E,E)*-FPP. For comparison, we include in our investigation a previously identified strictly trans-pathway specific germacrene A synthase NS1 from *Nostoc* sp. PCC 7120, which should not accept *(Z,E)*-FPP as a substrate [27].

FPP isomers and analogs have been used in studies with several sesquiterpene synthases to determine the mechanism of carbocation quenching [28–31] and the initial ionization and isomerization of *all-trans*-FPP for cis-trans-pathway specific enzymes [32–35]. However, most studies compared the kinetic properties of different FPP substrate geometrical isomers. Cyclization products of *(Z,E)*-FPP have only recently been investigated for several sesquiterpene synthase homologs from maize [36–38]. Here, we describe for the first time how substrate geometrical conformation determines the first cyclization event. Surprisingly and in contrast to previous studies with the maize enzymes, both Cop4 and Cop6 cyclize *(Z,E)*-FPP into products that are very different from those obtained with *(E,E)*-FPP. Most notably, cyclization of *(E,E)*-FPP and *(Z,E)*-FPP by Cop6 proceeds through opposite enantiomers of a β-bisabolyl cation intermediate.

Results

Kinetic parameters

Kinetic properties of the two fungal cis-trans pathway specific enzymes Cop4 and Cop6 and for comparison, the strictly trans-pathway specific germacrene A synthase from *Nostoc* sp. PCC 7120 (NS1) [27], were analyzed using purified recombinant proteins with *(E,E)*-FPP, *(Z,E)*-FPP and the 10-carbon *E*-GPP (trans geranyl diphosphate) as substrates.

Kinetic parameters were first determined with *(E,E)*-FPP (Table 1). Cop4 and Cop6 bind *(E,E)*-FPP with comparable affinity (K_m), but the catalytic turnover (k_{cat}) of Cop4 with this substrate is 70-fold lower than of Cop6, resulting in a catalytic efficiency (k_{cat}/K_m) for Cop4 that is almost two orders of magnitude lower than for Cop6. NS1 has a higher affinity (K_m) for *(E,E)*-FPP than the two fungal enzymes, while its catalytic turnover (k_{cat}) is only slightly higher than that of Cop4.

When *(Z,E)*-FPP was used as the substrate, only the cis-trans-pathway specific enzymes Cop4 and Cop6 show measurable activity, while expectedly no diphosphate release is detected in *in vitro* assays with the trans-pathway specific enzyme NS1 (Table 1). However, the activity of Cop6 with *(Z,E)*-FPP is too low for kinetic measurements. Cop4 on the other hand converts *(Z,E)*-FPP with a catalytic efficiency that is about 7-fold lower than with its natural substrate

(E,E)-FPP as the result of both a reduced substrate binding (40% higher K_m) and catalytic turnover (4-fold lower k_{cat}).

E-GPP is known to be converted by sesquiterpene synthases into monoterpenes [15,30,39–41]. Expectedly, all three enzymes accept *E*-GPP as a substrate, but the catalytic efficiency (k_{cat}/K_m) with the shorter prenyl-diphosphate substrate is lower compared to their longer FPP substrate (Table 1). *E*-GPP is a fairly good substrate for Cop6, which shows only a moderate reduction in K_m and k_{cat} compared to *(E,E)*-FPP. In contrast, the catalytic turnover (k_{cat}) of Cop4 and NS1 with *E*-GPP is more than two orders of magnitude lower compared to *(E,E)*-FPP.

Cyclization of *(E,E)*-FPP

To investigate further the differences in catalytic promiscuity previously observed in *E. coli* strains expressing Cop4 or Cop6, purified Cop enzymes (and purified NS1 for comparison) were incubated for 18 hrs with *(E,E)*-FPP and the resulting cyclization products were analyzed (Table 2, see Supplemental Figure 1 and 2 for GC chromatograms and mass spectra of product peaks, respectively).

Cop6 converts *(E,E)*-FPP with high selectivity into (−)-α-cuprenene (**3s**) which makes up 98% of the total sesquiterpenoids synthesized (see Supplemental Figure 3 for absolute configuration determination). In contrast, Cop4 cyclizes *(E,E)*-FPP into six different identified sesquiterpenes in addition to a number of unidentified sesquiterpenoid compounds. (−)-Germacrene D (**7s**) (see Supplemental Figure 4 for absolute configuration determination) and cubebol (**8s**) are the major products of Cop4, each making up about 30% of the total sesquiterpenoid compounds detected (see Scheme 1 for structures and corresponding compound numbers).

All sesquiterpenoids synthesized by both Cop4 and Cop6 from *(E,E)*-FPP involve rotation of the C2-C3 π bond of *(E,E)*-FPP to yield a cisoid neryl cation intermediate that is rearranged and finally quenched along different routes (Scheme 1). Previous studies by Cane's group with trichodiene synthase [42] and more recently with epiisozizane synthase [43] have established that ionization and isomerization of *(E,E)*-FPP generates the (*3R*)-NPP intermediate. Subsequent ionization and 1,6-cyclization then yields a (*6R*)-bisabolyl cation which in the case of trichodiene synthase is further rearranged into a (*7R*)-cuprenyl cation to yield trichodiene after a final methyl shift [44]. The finding that Cop6 cyclizes (*E,E*)-FPP to (−)-α-cuprenene (**3s**) and also converts NPP into α-cuprenene, albeit with noticeably reduced selectivity (Supplemental Figure 5A), suggests that Cop6 follows a cyclization pathway similar to that of trichodiene synthase until the final methyl shift. Hence, the reaction pathway shown in Scheme 1 assumes that the absolute configuration of NPP is (*3R*). Cop4 is also able to cyclize NPP and yields the same products obtained with (*E,E*)-FPP, except for one new major compound (**18s**) that could not be identified (Supplemental Figure 5B and Supplemental Figure 2 for mass spectrum). In the case of Cop4, ionization and 1,10-cyclization of the (*3R*)-NPP intermediate gives a (*Z,E*)-germacradienyl cation that upon 1,3-hydride shift and deprotonation yields (−)-germacrene D. Additional hydride shifts and ring closures produce the other cyclization products detected in the Cop4 reaction. Assuming that the configuration of the isopropyl group in (−)-germacrene D is maintained; we can postulate the reaction mechanism shown in Scheme 1.

The trans-pathway specific enzyme NS1 also generates a germacradienyl cation but with the C2-C3 π bond remaining in a trans-configuration. This enzyme is as selective as Cop6 in the cyclization of *(E,E)*-FPP and synthesizes mostly germacrene A (**1s**) (93.5%, detected as its heat induced Cope-rearrangement product β-elemene [27]) (Table 2,Scheme 1). The *4Z*-isomer

of germacrene A, helminthogermacrene A (6.5%, detected as its Cope-rearrangement product *cis*-β-elemene [45]) is produced by NS1 as a minor cyclization product.

Cyclization of *(Z,E)*-FPP

(Z,E)-FPP yields after diphosphate cleavage directly a cisoid farnesyl cation intermediate. Hence, no isomerization step precedes initiation of the subsequent carbocation rearrangement reactions. Although *(Z,E)*-FPP has been used as a surrogate substrate for cis-trans pathway specific enzymes for kinetic measurements[33,36–38,46], only a few recent examples analyzed the cyclization products of *(Z,E)*-FPP [36–38] and found them to be comparable to those obtained with the *all-trans*-FPP isomer. We sought to determine whether cyclization of the *cis*-FPP geometrical isomer by Cop4 and Cop6 would similarly yield the same product profiles and selectivities observed with their normal substrate *(E,E)*-FPP.

In contrast to the previous studies [36–38], Cop4 and Cop6 generated very different cyclization products with the *cis*-FPP isomer compared to the compounds made with the all-trans isomer *(E,E)*-FPP. Moreover, the high product selectivity observed for Cop6 with *all-trans*-FPP is not any longer obtained with the *cis*-FPP isomer (Table 2, see Supplemental Figure 1 and 2 for GC chromatograms and mass spectra of product peaks, respectively). Cop4 catalyzes the cyclization of *(Z,E)*-FPP into α–acoradiene (**11s**) as the major product and four other significant sesquiterpenoid products (**14s**, **15s**, **16s**, **17s**) (see Scheme 2 for structures and compound names). By determining the absolute configuration of cadina-4,11-diene (**14s**) produced by Cop4 with a cadina-4,11-diene standard with a known configuration (in *Amyris balsamifera* essential oil [47], Supplemental Figure 6), the absolute configurations of the other Cop4 products shown in Scheme 2 can be postulated, assuming that stereocenters introduced in the cyclization reaction are maintained until product release by the enzyme. Cop4 also makes a number of unidentified minor products accounting for 23.7% of all sesquiterpenoid products detected.

Cop6 converts *(Z,E)*-FPP into a smaller and different set (except for α-acoradiene (**11s**) and amorpha-4,11-diene (**12s**)) of cyclization products compared to Cop4 (Table 2). The major Cop6 product (**10s**), representing 45% of the total terpenoid products, could not be identified. The mass spectrum of this unidentified compound does not yield a complete match with published reference spectra, although its fragmentation pattern suggests it to be structurally related to α-acoradiene (**11s**) (Supplemental Figure 2). Differences in retention times after chiral GC-MS separation of α-acoradiene (**11s**) and amorpha-4,11-diene (**12s**) produced by Cop6 and by Cop4 (Supplemental Figure 6) show that conversion of *(Z,E)*-FPP by the two enzymes yields cyclization products with opposite absolute configuration. Knowing the absolute configuration of cadina-4,11-diene (**14s**) produced by Cop4, we can postulate the Cop6 reaction mechanism shown in Scheme 2.

Cyclization of *(Z,E)*-FPP by Cop4 and Cop6 can be rationalized to proceed through a β-bisabolyl cation, which is supported by the detection of β-bisabolene (**16s**) as a cyclization product of *(Z,E)*-FPP by Cop4. The detection of α-acoradiene (**11s**) and amorpha-4,11-diene (**12s**) as cyclization products of *(Z,E)*-FPP (Table 2) suggests that the cyclization of this FPP isomer by Cop4 and Cop6 proceeds through a (*6S*)-β-bisabolyl cation intermediate [41,48] rather than through a (*6R*)-β-bisabolyl cation as in the cyclization of *(E,E)*-FPP by Cop6. The two enzymes then catalyze a 1,2-hydride shift yielding a second cation with opposite configuration at C7 ((*7S*)-cation in the case of Cop6 and (*7R*)-cation in the case of Cop4) which give rise to cyclization products with different absolute configurations. Deprotonation yields α-acoradiene (**11s**) while an additional 1,2-hydride shift leads to different isomeric carbocation intermediates *en route* to the products **17s**, **15s** and **14s** [29] (Scheme 2).

To verify the proposed reaction mechanism via a (*6S*)-β-bisabolyl cation intermediate, we first determined by chiral GS-MS with authentic reference compounds the stereochemistry of β-bisabolene (**16s**) produced by Cop4 as a minor compound after premature deprotonation of the corresponding cation intermediate. Figure 1A shows that Cop4 makes (*6S*)-β-bisabolene (**16s**), confirming the *6S*-stereocenter of the β-bisabolyl cation.

Because Cop6 does not catalyze the premature deprotonation of the β-bisabolyl cation with either FPP isomer under the reaction conditions used (18 hrs incubation), a mutation, N224D, was introduced into the active site of Cop6. An analogous mutation is known to increase the premature deprotonation of the β-bisabolyl cation in trichodiene synthase [48]. Mutant Cop6N224D now makes a small amount of an additional compound that was identified by chiral GS-MS as (*6S*)-β-bisabolene (**16s**) (Figure 1B). Interestingly, the active site mutation N224D does not affect the product profile of Cop6 with its normal substrate *(E,E)*-FPP.

Cyclization of *E*-GPP

Results from kinetic studies with Cop6, Cop4 and NS1 show that *E*-GPP is converted by all three enzymes but with very different catalytic efficiencies (Table 1). The shorter isoprene chain of *E*-GPP is expected to exhibit a higher degree of conformational freedom in the active site of sesquiterpene synthases compared to *(E,E)*-FPP. Consequently, Cop6 is expected to produce multiple products with *E*-GPP instead of one with *(E,E)*-FPP. Because cyclic monoterpenes can only be produced by terpene synthases that can isomerize the C2-C3 π bond of *E*-GPP [49,50], only Cop4 and Cop6 but not NS1 are expected to cyclize *E*-GPP.

To confirm our expectations purified enzymes were incubated for 18 hrs with *E*-GPP and products analyzed (Table 2, see Supplemental Figure 7 and 8 for GC chromatograms and mass spectra of product peaks, respectively). Cop4 and Cop6 convert *E*-GPP into both acyclic (**1m, 2m, 3m**) and cyclic (**4m, 5m, 6m**) monoterpenes (Table 2,Scheme 3 and Supplemental Figure 7). However, cyclization of *E*-GPP is more efficiently catalyzed by Cop6 compared to Cop4. Cop6 accumulates limonene (**4m**) (45% of total terpene products) as the major product while Cop4 makes mostly the acyclic terpene (*E*)-β-ocimene (**1m**) (57.6% of total terpene products) (Table 2, Scheme 3). The strictly trans-pathway specific sesquiterpene synthase NS1 converts *E*-GPP as expected exclusively into acyclic monoterpene olefins, with linalool as the major product (**3m**).

Influence of reaction conditions on product profiles

We noted that the product profile of Cop4, unlike Cop6, measured in the head-space of recombinant *E. coli* cultures [24,25] (major product δ-cadinene (**9s**) is different compared to the product profile obtained *in vitro* in this study (Table 2, (−)-germacrene D (**7s**) and cubebol (**8s**) major products). This may suggest that the cyclization reaction catalyzed by Cop4 is susceptible to changes in the reaction environment. To test this, conversion of *(E,E)*-FPP by Cop4 and Cop6 was analyzed under different reaction conditions.

Changes in reaction conditions were found to influence the product profiles of Cop4 and Cop6 strikingly differently. Remarkably, Cop6 does not change its product profile under any of the condition tested and always converts *(E,E)*-FPP highly selective into greater than 98% of α-cuprenene as shown in Table 2. The product profile of Cop4 on the other hand is dependent on the reaction condition used and certain conditions dramatically change its catalytic fidelity (Table 3).

Changing the ionic strengths of the reaction by adding 1 M NaCl does not affect the product specificity of Cop4 significantly (Table 3), although generation of (−)-germacrene D (**7s**) decreases somewhat in favor of cubebol (**8s**), which is located further downstream on the

cyclization path (Scheme 1). In addition, the fraction of sesquiterpene olefins that could not be structurally identified increases with increasing ionic strength.

Lowering the reaction temperature from 25 to 4 °C increased the selectivity of Cop4 for (−)-germacrene D (**7s**) and decreased the fraction of structurally unidentified sesquiterpene olefins by half (Table 3). Increasing the reaction temperature to 37 °C, however, had the opposite effect and decreased the fidelity of Cop4. At this temperature Cop4 generated a relative larger fraction of products (β-cubebene (**4s**), sativene (**5s**) δ-cadinene (**9s**) and β-copaene (**5s**)) that are derived from a cadinyl cation intermediate.

The product specificity of terpene synthases is known to be influenced by the type of metal cofactor bound by the enzyme [38,40,51]. The first notable feature of Cop4 product profiles obtained in reactions where Mg^{2+} is replaced with either Mn^{2+} or K^{+} is the disappearance of β-copaene (Table 3). In the presence of the divalent cation Mn^{2+}, Cop4 favors a reaction path that ends after one cyclization in (−)-germacrene D (**7s**). A larger fraction of sesquiterpene olefins that could not be structurally identified is also produced by Cop4 in the presence of Mn^{2+}. The monovalent K^{+} decreases the (−)-germacrene D (**7s**) yield and instead increases the overall yield of tricyclic sesquiterpene olefins (**4s, 5s** and **6s**).

The most dramatic effect on the product spectrum of Cop4 was obtained by altering the pH of the reaction (Table 3 and Figure 2). Under both alkaline and acidic conditions Cop4 becomes a very selective enzyme with only one major product (**7s**) compared to the three major compounds (**7s**, **8s**, **9s**) produced under neutral reaction conditions. At pH 10, the cyclization reaction ends with the hydride shift and deprotonation of the germacradienyl cation to yield (−)-germacrene D (**7s**) (91% of total sesquiterpene products), while at pH 5.0 cyclization can proceed via a 1,6 ring closure to also yield a small amount of δ-cadinene (**9s**) (12% of total sesquiterpene products) in addition to (−)-germacrene D (**7s**).

Structural modeling

Structural models for Cop4 and Cop6 were built to understand the differences observed in their catalytic fidelities. Models in the open (no substrate and Mg^{2+} bound) and closed (Mg^{2+} and pyrophosphate (PPi) bound in the active site) conformation were built using the structure of trichodiene synthase from *F. sporotrichoides* [48,52] for Cop6 and of aristolochene synthase from *A. terreus* [20] for Cop4. The generated models for Cop4 and Cop6 are in very good agreement with their respective templates and conformational differences observed between the open and closed template crystal structures are also reflected in the two models.

Hydrogen bond interactions and metal ion coordination in the PPi bound closed conformation of the Cop models were compared to their template structures (Figure 3A and 3B). Residues of the two conserved motifs (DDXXD, NSE/DTE) and basic motif (RY) participating in the coordination of the $Mg^{2+}{}_3$-PPi complex in trichodiene synthase and aristolochene synthase are in perfect alignment with corresponding residues in the two Cop models; although M228 in Cop4 cannot make an ionic interaction with PPi as does the equivalent residue K226 in aristolochene synthase. The three Mg^{2+} ions assume similar positions in the two Cop models, but the PPi is rotated by 180° in the Cop4 binding pocket. Residue R304 in trichodiene synthase and residue R302 in the Cop6 model form a charge-charge interaction with the second aspartate residue in the conserved DDXXD motif (D103 and D101 in Cop6 and trichodiene synthase respectively). The corresponding residues in Cop4 (E88) and aristolochene synthase (E94), however, are not positioned to form a similar interaction.

Comparison of the active site cavities of the Cop4 and Cop6 models in the open conformation shows that Cop4 has a much larger binding pocket compared to the narrow active site cleft seen in the Cop6 model (Figures 3C and 3D). The binding pocket of the Cop4 model is much

larger with more space at the cavity bottom compared to its template structure, aristolochene synthase. The active site clefts of the Cop6 model and trichodiene synthase, however, are comparable. Volume calculations using CASTp indicate an active site cavity volume for Cop4 of 3376 $Å^3$ that is twice that measured for Cop6 (1695 $Å^3$), trichodiene synthase (1740 $Å^3$) and aristolochene synthase (1742 $Å^3$). The trinuclear Mg^{2+} cluster and the liganded PPi of the substrate form a plane at the entrance of the binding pocket while the isoprenoid chain extends into the binding cavity. The much larger active site cavity of Cop4 suggests that its binding pocket can accommodate multiple isoprenoid chain conformation, thus explaining the larger number of cyclization products obtained with this enzyme.

Superimposition of the Cop models with their respective fungal template structures (Figure 3E) shows that all four terpene synthases share the same α-helical fold with six helices surrounding the active site cavity. A notable difference between the four structures is the length of the loop (H-α-1 loop in trichodiene and aristolochene synthase [20, 53]) that caps the active site in the liganded, closed enzyme conformation. In the trichodiene synthase structure and Cop6 model, this loop is shorter compared to the other structures. Aristolochene synthase has a particularly long and flexible loop that is disordered in the open conformation. A comparison of the primary sequence of the loops shows that five out of nine residues in the Cop4 loop are basic resulting in a localized positive charge at the entrance of the binding pocket under neutral pH conditions (Figure 3E). The loop of Cop6 on the other hand is composed of mostly acidic and hydrophobic residues.

Discussion

Cop4 and Cop6 have divergent product selectivities and cyclize *(E,E)*-FPP via a (*6R*)-bisabolyl cation to different products

The analysis of *(E,E)*-FPP conversion performed in this study with purified enzymes confirms the broad product selectivity of Cop4 and the high selectivity of Cop6 previously observed in recombinant *E. coli* cultures (Table 2). However, while δ-cadinene (**9s**) is the major product of Cop4 in *E. coli*, (−)-germacrene D (**7s**) and cubebol (**8s**) are the major compounds made by Cop4 *in vitro*.

The proposed reaction mechanism for *(E,E)*-FPP cyclization by Cop4 involves the 1,10-cyclization of a cisoid neryl cation to form a *(Z,E)*-germacradienyl cation, which undergoes a 1,3-hydride shift to form an allylic carbocation that is either deprotonated to yield (−)-germacrene D (**7s**), the major product of Cop4, or 1,6 cyclized to the bicyclic cadinyl cation (Scheme 1). Deprotonation of this cation would produce δ-cadinene (**9s**), while 1,2-hydride shift followed by 2,6-ring closure and quenching of the ensuing carbocation with H_2O yields the tricyclic cubebol (**8s**) as the second major product of Cop4. Labeling studies with deuterated *(E,E)*-FPP and reactions with (*3R*)-NPP using a recombinant sesquiterpene synthase from cotton have confirmed that δ-cadinene biosynthesis requires the isomerization *(E,E)*-FPP [28,32]. A similar mechanism via (*3R*)-NPP has also been described for the synthesis of (−)–germacrene D by germacradienol/germacrene D synthase from *Streptomyces coelicolor* [54]. It should be noted that (−)-germacrene D can also be derived from the *(E,E)*-germacradienyl cation [55,56], but cyclization products derived from a cadinyl cation bearing a C2-C3 π bond in cis-configuration require the isomerization of *(E,E)*-FPP.

Unlike Cop4, Cop6 makes almost exclusively (−)-α-cuprenene (**3s**) (98%). Comparable selectivities for their major terpene products have been reported for trichodiene synthase (89%) [48], aristolochene synthases from *A. terreus* (>99%) and *P. roqueforti* (94%) [57] and δ-cadinene synthase from cotton (98%) [32]. The proposed reaction mechanism for the cyclization of *(E,E)*-FPP to (−)-α-cuprenene by Cop6 (Scheme 1) following the same cyclization route described for trichodiene synthase until the formation of the (*7R*)-cuprenyl

cation [13,33,42], at which point wild-type trichodiene synthase continues carbocation rearrangement while Cop6 and some trichodiene synthase mutants [35,44,48,58] quench the carbocation to form (−)-α–cuprenene. Specifically, Cop6 and trichodiene synthase first generate a (*6R*)-β-bisabolyl carbocation from a cisoid neryl cation following 1,6-ring closure. A second 11,7-ring closure and 1,4-hydride shift then yields the (*7R*)-cuprenyl cation which is deprotonated by Cop6, while trichodiene synthase catalyzes two additional methyl shifts prior to deprotonation.

The remarkable differences in product selectivity observed with Cop4 and Cop6 correlate with the different sizes of their active sites. While, Cop6 has a relative narrow active site cleft that likely binds *(E,E)*-FPP with high accuracy in one cyclization competent conformation, the large active site cavity of Cop4 allows a much higher degree of conformational freedom for cyclization intermediates, giving rise to multiple alternative cyclization pathways. Interestingly, the larger binding pocket of Cop4 does not support the 1,6-cyclization of (*3R*)-NPP to the β-bisabolyl cation, although this monocyclic cyclization product with its flexible isoprenoid tail is accommodated in the much smaller active site cleft of Cop6. Instead, Cop4 exclusively catalyzes the 1,10 cyclization of the proposed (*3R*)-NPP intermediate and multiple reaction pathways become possible only after this initial cyclization step. Similar product diversification after initial farnesyl cation cyclization is also observed for other terpene synthases [14,59,60], while for instance, γ-humulene synthase catalyzes different ring closures of a cisoid neryl cation [15].

Both the high-fidelity enzyme Cop6 and the promiscuous Cop4 bind *(E,E)*-FPP with comparable affinity (Table 1), but the catalytic turnover of Cop4 is about 70-fold lower than the k_{cat} of Cop6. The steady-state kinetic properties of Cop4 suggest that it binds *(E,E)*-FPP with high affinity in one selective conformation that yields the *(Z,E)*-germacradienyl cation. Once this carbocation is formed, multiple conformations, including unproductive cyclization conformations, may become possible, thus reducing the overall catalytic efficiency of this enzyme.

(Z,E)-FPP is cyclized by Cop4 and Cop6 via a (*6S*)-β-bisabolyl cation intermediate

(Z,E)-FPP has been used as surrogate substrate for sesquiterpene synthases that isomerize the C2-C3 π bond of *(E,E)*-FPP to form a cisoid neryl cation [33,36–38,46]. Cop4 catalyzes the cyclization of the *cis*-FPP isomer with only a modestly reduced binding affinity (K_m) and catalytic turnover (k_{cat}) (Table 1), suggesting that its large active site cavity can readily accept the sterically more demanding *cis*-FPP isomer. Cop6 on the other hand shows measurable activity with *(Z,E)*-FPP only after prolonged overnight incubation, suggesting that the *cis*-FPP isomer cannot easily be accommodated by its narrow active site cleft. Nevertheless, Cop6 can catalyze diphosphate cleavage of *(Z,E)*-FPP to initiate subsequent cyclization reactions. The strictly trans-pathway specific enzyme NS1 expectedly does not convert *(Z,E)*-FPP because it either is unable to bind *(Z,E)*-FPP or catalyze diphosphate cleavage.

Very few studies have compared the cyclization products obtained with the two FPP geometrical isomers, although pioneering work by Croteau's group on the cyclization mechanism of monoterpene synthases investigates the cyclization products obtained with *E*-GPP and *Z*-GPP [49,61,62]. Recent studies with sesquiterpene synthases TPS4, TPS6 and TPS11 from maize report comparable product profiles with both FPP isomers [36–38]. An enzyme preparation from the liverwort *Heteroscyphus planus* [46] converted *(E,E)*-FPP and *(Z,E)*-FPP to different isomeric cadinanes, but the cyclization paths of the two FPP substrates diverge only after 1,10-cyclization of the cisoid farnesyl cation intermediate. The maize enzymes and the liverwort enzyme preparation therefore appear not to discriminate between *(E,E)*- or *(Z,E)*-FPP when it comes to generation and cyclization of the first cisoid allylic carbocation intermediate. Cop4 and Cop6, however, yield very different products with *(E,E)*-

and *(Z,E)*-FPP. As discussed below, the two Cop enzymes must bind the two geometrical isomers as different conformers resulting in the generation of opposite enantiomers of the first cyclic cation intermediate. This has not been observed before and it remains to be seen whether other cis-trans pathway specific sesquiterpene synthase show the same discrimination between the two geometrical FPP isomers like Cop4 and Cop6 or generate the same products with both isomers like the maize enzymes [36–38].

In detail, Cop4 catalyzes a 1,10-ring closure of a cisoid neryl cation derived from its normal substrate *(E,E)*-FPP. But Cop4, is despite its large active site cavity, unable to catalyze the same cyclization reaction with a cisoid carbocation derived from *(Z,E)*-FPP. Instead Cop4 now catalyzes a 1,6-ring closure to generate a β-bisabolyl cation intermediate from *(Z,E)*-FPP (Table 2, Scheme 2).

Remarkably, Cop6 cyclizes *(Z,E)*-FPP through a (*6S*)-β-bisabolyl cation intermediate rather than the (*6R*)-β-bisabolyl cation postulated for Cop6 with *(E,E)*-FPP. Cop4 also cyclizes *(Z,E)*-FPP through a (*6S*)-β-bisabolyl cation intermediate. This means that the *cis*-FPP isomer must bind as the right-handed helical conformer in the active sites of the Cop enzymes, while the normal trans-FPP substrate must bind as the left handed helical conformer in the two active sites to explain the different stereochemistries seen in the cyclization pathways of the two FPP substrates [50].

FPP adopts an extended conformation in solution [63], but the active site of a terpene synthase must bind FPP in a helical conformation to facilitate cyclization. It is obvious that the conformation of the substrate in the active site controls the stereochemical course of the cyclization reaction. Crystallographic studies of aristolochene synthase and fluorinated FPP analogs suggest that binding of the substrate diphosphate moiety to the trinuclear magnesium cluster triggers active site closure and controls the conformation of the FPP substrate in the active site [64]. The diphosphate moiety of different substrates/analogs will likely be bound in the same orientation independently of its relative position in the isoprenoid chain of different substrates. Hence, the relative position of the diphosphate group in the substrate will determine the positioning of the isoprenoid moiety in the active site of each terpene synthase. Because the diphosphate group is positioned differently in *(Z,E)*-FPP compared to *(E,E)*-FPP, it is safe to assume that the isoprenoid chain of the two FPP geometrical isomers adopt different binding conformations in the active sites of Cop4 and Cop6. Alternatively or in addition, isomerization of *(E,E)*-FPP may control the binding conformation of the isoprenoid chain as it has been demonstrated for limonene synthase using different substrate isomers [65]. In contrast, maize terpene synthase TPS4 not only cyclizes *(E,E)*-FPP and *(Z,E)*-FPP to similar products, but appears to bind each geometrical isomer both in the right- and left handed conformations, resulting in cyclization products that are derived from both the (*6S*)- and (*6R*)-β-bisabolyl cation intermediate [37]. A structural model of this sesquiterpene synthase suggests that its active site cavity has two binding pockets that can accommodate the two different β-bisabolyl cation enantiomers [37]. The structural models of Cop4 and Cop6 do not indicate the existence of two active site binding pockets.

Cop4 and Cop6 convert *E*-GPP into cyclic and acyclic monoterpenes

Sesquiterpene synthases are known to accept *E*-GPP as a substrate to produce monoterpenes [15,30,39–41]. All three enzymes tested in this study expectedly catalyze the conversion of *E*-GPP into different monoterpenes (Table 1). Cop4 binds *E*-GPP with a much reduced affinity compared to both FPP isomers. Its large binding cavity most likely does not provide a good fit for binding of the shorter substrate in a productive conformation. Cop6, on the other hand, can convert *E*-GPP with only a moderately reduced efficiency compared to *(E,E)*-FPP, but its fidelity suffers with this non-natural substrate, resulting in the generation of multiple products

(Table 2, Scheme 3). In contrast to *(E,E)*-FPP, *E*-GPP likely adopts multiple conformations in the enzyme's binding pocket causing different catalytic outcomes.

Studies with monoterpene synthases have shown that only terpene synthases that can isomerize the C2-C3 π bond of *E*-GPP can make cyclic monoterpenes [49,50]. Likewise, only sesquiterpene synthases known to isomerize the C2-C3 π bond of *(E,E)*-FPP have been reported to synthesize cyclic products from *E*-GPP [15,30,39–41]. In this study, only Cop4 and Cop6 produce monocyclic monoterpene olefins (**4m**, **5m**, **6m**), while the strictly trans-pathway specific enzyme NS1 only makes acyclic monoterpenes (**1m**, **2m**, **3m**). The absence of any detectable cyclic products with NS1 confirms its inability isomerize the C2-C3 π bond of allylic isoprenoid diphosphate substrates.

The acyclic monoterpenes (*Z*)-β-ocimene (**1m**) and linalool (**3m**) make up more than 90% of the monoterpenes produced by NS1 (Table 2). Their formation can be rationalized to originate from a transoid, endo-conformation of the geranyl cation, while the minor NS1 cyclization product (*E*)-β-ocimene (**2m**) originates from a transoid, exo-conformation of the bound prenyl-chain [49]. The same monocyclic terpenes can also be obtained from a cisoid geranyl cation (neryl cation), where the exo-conformation would now yield **1m** and **3m**, while the endo-conformation would give **2 m**. Cop4 and Cop6 convert 30% and 50%, respectively, of *E*-GPP into cyclic monoterpene products (Table 2). With both enzymes, limonene (**4m**) is synthesized as the major cyclic monoterpene product. Limonene can be derived from either a cisoid, exo- or cisoid, endo-conformation of the initial geranyl cation [49]. The accumulation of **1m** (Cop4) and of **1m** and **3m** (Cop6) as major acyclic products by the two Cop enzymes, suggests that the cisoid geranyl cation is likely predominantly bound in an *exo*-conformation which yields both acyclic and cyclic products.

Reaction conditions strongly influence the product profile of Cop4 but not of Cop6

A major determinant for product selectivity is the degree of conformational flexibility that the substrate possesses in the active site of a terpene synthase. Hence, Cop6 with its narrow binding pocket is a high fidelity enzyme, while the large cavity of Cop4 yields multiple cyclization products (Table 2). Consequently, by modifying the conformational flexibility and/or fit of the bound substrate in the active site, the fidelity of the cyclization reaction may be altered. This can be done by protein engineering or modifying the physical environment of an enzyme. While there are many examples that use protein engineering to explore the catalytic promiscuity of terpene synthases [7,9], only very few studies have investigated how reaction conditions affect the fidelity of terpene synthases [9,38,40,51,66,67].

In this study we have compared the effects that different reaction conditions have on the cyclization fidelity of Cop4 and Cop6. As expected, the product profile of Cop6 never changed in response to any of the conditions tested, because its active site must provide a rigid template for binding of *(E,E)*-FPP in an optimal conformation (Table 2). The product profile of the low-fidelity Cop4 in contrast was easily altered by varying reaction conditions (Table 3, Figure 2).

Substitution of Mg^{2+} with Mn^{2+} as the divalent metal ion shifts the product profile of Cop4 to germacrene D, disfavoring subsequent ring closures that would produce the cadinyl cation and its tricyclic descendents (Scheme 1). The larger size of the Mn^{2+} ion has been suggested to reduce the size of the active site of terpene synthases and thus, change the conformational flexibility of the bound substrate [68]. The product selectivity of amorphadiene-4,11-diene synthase increased from 80% to 90% for amorphadiene in the presence of Mn^{2+} [68]. In other examples, replacement of Mg^{2+} with Mn^{2+} increases premature quenching of carbocation intermediates [38,40].

Because temperature influences both protein (and hence, flexibility of the active site) as well as prenyl chain motion, product fidelity is expected to decrease with increasing temperature. A modest decrease in catalytic fidelity at higher reaction temperature has been observed with epi-aristolochene synthase [9]. Temperature has a much more pronounced effect on the cyclization fidelity of Cop4 (Table 3).

The most notable and dramatic effect on the catalytic fidelity of Cop4 enzyme was obtained when enzyme reactions are carried out under alkaline (pH 10) or acidic (pH 5.0) conditions. Under both conditions, Cop4 becomes a very selective germacrene D synthase (Table 3, Figure 2). At pH 10, none of the cadinyl cation derived products at pH 8 are present in the reaction. The strong effect of pH on product selectivity seen with Cop4 is in contrast to what has been observed with amorphadiene-4,11-diene synthase [68]. The product selectivity of this enzyme was not influenced by the surrounding pH, which was explained by supposing that the loop covering the active site in the closed conformation will completely shield the active side from outside solvent effects. The product selectivity of Cop6 also is not affected by the pH of the reaction. Apart from the size of their active sites, Cop4 and Cop6 show differences in their loops that are supposed to cover the active site upon substrate binding. In contrast to Cop6 (and also to trichodiene and aristolochene synthase), Cop4 contains a larger number of basic amino acid residues in its loop (Figure 3E). The histidine side chain in the Cop4 loop, in particular, will have a strong impact on the net charge of the loop at different pH values. Changes in its net charge will impact interactions with residues of the active site entrance and thus may influence protein conformation and consequently, diphosphate binding, positioning and ionization of the substrate in the binding pocket. Mutagenesis studies have so far largely been focused on residues lining the active site entrance that are directly involved in coordinating the trinuclear Mg^{2+} cluster and binding of the substrate diphosphate [13,34,35,48,53]. The results obtained in this work with Cop4 suggest that this lid may play an important role in catalysis. Additional mutagenesis studies in the lid regions of terpene synthases are necessary to define their functions and explore whether changes in this region impact the catalytic promiscuity of terpene synthases.

Conclusions

In this work we describe the reaction mechanism of two new fungal sesquiterpene synthases that both isomerize the C2-C3 π bond of *(E,E)*-FPP *via* an NPP intermediate prior to catalysis of subsequent cyclization reactions. We show that Cop6 is a high fidelity enzyme while Cop4 is very promiscuous, generating multiple cyclization products from *(E,E)*-FPP. The fidelity of Cop6 with *(E,E)*-FPP can be attributed to the enzymes' narrow active site which restricts binding of *(E,E)*-FPP to one cyclization competent conformation. In contrast, the promiscuous Cop4 has a large active site cavity that allows binding of *(E,E)*-FPP in several cyclization competent conformations.

We demonstrate that the promiscuity of Cop4, but not of Cop6, is strongly influenced by reaction conditions. Changing the pH of the reaction dramatically changed the product profile of Cop4, converting the enzyme from a very promiscuous sesquiterpene synthase into a high fidelity enzyme. Such a dramatic effect of reaction condition on the product profile of a terpene synthase has not been reported previously. Inspection of the Cop4 structural model and comparison with structures of other fungal sesquiterpene synthases and the Cop6 model suggests that the amino acid residues of the loop that covers the active site of terpene synthases may be important in determining the cyclization products of sesquiterpene synthases. Hence, mutating the loop region of terpene synthase may be a different strategy for engineering of terpene synthases with desired product profiles. Studies are underway to test this approach with different terpene synthases.

Finally, by analyzing the cyclization products generated by Cop4 and Cop6 with the two geometrical isomers of FPP, we show for the first time that the two FPP isomers must be bound as different helical conformers in the active sites of Cop4 and Cop6 to rationalize the different cyclization products obtained with each FPP isomer. This observation is in contrast to the results obtained with maize terpene synthases [37], which produce the same products with either FPP isomer. However, these plant enzymes seem to have two FPP binding pockets in their active site that can accommodate both helical FPP conformers, while the two Cop enzymes like many other cis-trans pathway specific enzymes have only one binding pocket. Studies with other cis-trans pathway enzymes to determine the cyclization products with both geometrical isomers of FPP should confirm our observations.

Experimental Section

Chemicals

(E,E)-FPP and *E*-GPP were purchased from Sigma-Aldrich (St. Louis, MO). *(Z,E)*-FPP was synthesized from *(E,E)*-farnesol as described by Shao et al.[69] DNA modifying enzymes were obtained from New England Biolabs (Ipswich, MA). (*6S*)- and (*6R*)-β-bisabolene standards were gifts from Prof. Jörg Degenhardt, Max Planck Institute for Chemical Ecology, Jena, Germany. α–Cuparene (98% (+)-enantiomer) was obtained from Chromadex (Irvine, CA). Other chemicals were from suppliers as described or from Sigma-Aldrich. Nerolidol was purchased from Sigma Aldrich and phosphorylated according to the method of Popjak et al. [70] with one modification. After all the ditriethylamine phosphate was added and left stirring for 2 hours, the crude reaction mixture was purified via RP-HPLC (Solvent A: H_2O in 0.1% trifluoroacetic acid, Solvent B: acetonitrile in 0.1% trifluoroacetic acid, Gradient: 0% B over 5 min, 0–60% B over 25 min, 60–100% B over 5 min). Nerolidyl diphosphate elutes at 42% B and was subsequently lyophilized to give a white powder. Such powder was dissolved in 30:70 methanol:water at 1 mM final concentration.

Strains and growth conditions

E. coli strain JM109 was used for cloning and recombinant proteins were expressed *E. coli* strain BL21 (DE3). *E. coli* cultures were grown in Luria-Bertani (LB) medium supplemented with appropriate antibiotics ampicillin (100 μg mL^{-1}) or kanamycin (30μg mL^{-1}) at 30 °C, 250 rpm.

Gene cloning

Genes encoding Cop6 and Cop4 were subcloned from their respective pUCmod plasmids [24,25] into the *Nde*I and *Not*I sites of pHIS8 [71], in the case of Cop6, and into the *Nde*I and *Xho*I of pET21b (Novagen), in the case of Cop4, for overexpression under the control of the T7 promoter. Cop4 and Cop6 are expressed with a 6x histidine tag (pET21b-Cop4) or 8x histidine tag (pHIS8-Cop6) added to their N-terminus. Cloning of NS1 into the expression vector pET21b (pET-NS1) is described in [27]. The Cop6 N224D mutant was obtained by overlap extension PCR using mutagenic forward and reverse oligonucleotide primer. The PCR product was digested with *Nde*I and *Not*I for cloning into plasmid pHIS8.

Protein expression and purification

Expression vectors pHIS8-Cop6 and pET21b-Cop4 were transformed into *E. coli* BL21 (DE3). For protein overexpression, a 50 mL culture was inoculated with 1 mL of an overnight culture and grown at 30 °C until it reached an OD_{600} of 0.6 at which point protein expression was induced by the addition of 1 mM IPTG and cultivation was continued for 18 hrs at 30 °C. Cells were harvested by centrifugation and stored at −20 °C until used. For protein purification, harvested cells were resuspended in terpene synthase buffer (10 mM Tris-HCl, 10 mM

$MgCl_2$ and 1 mM β-mercaptoethanol at pH 8.0) and sonicated. Cell debris was cleared by centrifugation and the cleared protein extract was purified by metal affinity chromatography. Soluble protein was loaded onto a Talon Resin (Invitrogen, Carlsbad, CA) equilibrated with terpene synthase buffer containing 10 mM imidazole. Following protein binding to the column, the column was washed three times with terpene synthase buffer containing 20 mM imidazole prior to elution with 300 mM imidazole. Overexpression and purification of recombinant sesquiterpene synthase NS1 followed the same procedure previously described in [27]. Protein concentrations were determined using Bradford reagent (BioRad, Hercules, CA).

Kinetic parameters

Steady-state kinetics of sesquiterpene synthases (Cop6, Cop4 and NS1) were determined with varying concentrations (1–100 μM) of prenyl diphosphate substrates (*(E,E)*-FPP, *(Z,E)*-FPP and *E*-GPP) by measuring the release of pyrophosphate (PPi) as described in [27]. Briefly, PPi was detected using a coupled enzyme system consisting of PPi-dependent fructose-6-phosphate kinase, aldolase, triosephosphate isomerase and α-glycerophosphate dehydrogenase. The enzymes are supplied as pyrophosphate reagent by Sigma-Aldrich (product number P7275) and were reconstituted in assay buffer prior to use (16.7 mg in 1 mL terpene synthase buffer). PPi released is measured by the consumption of NADH, resulting in a decrease in absorbance at 340 nm. Microplate assays were carried out with 50 μL of pyrophosphate reagent, 90 μL of assay buffer and 10 μL of varying concentrations of different substrates. Blank reactions without substrate were run in parallel. Assay mixtures were allowed to equilibrate for 5 min at 30 °C prior to the addition of 5 μL of enzyme (0.2 mg mL^{-1}) to start the reaction. The activity was determined as the difference between the decrease of absorbance per minute of the sample and of the blank. Using an extinction coefficient for NADH of $\varepsilon_{340\ nm} = 6.22 \times 10^3\ M^{-1}\ mL^{-1}$, one unit of activity was defined as the amount of enzyme needed to release 1 μmol of PPi, inducing the consumption of 2 μmol of NADPH. The K_m and V_{max} values were determined non linear fit of V vs [S] plot. The analysis was carried out running a macro in Xcel 2007.

In vitro analysis of sesquiterpene product profiles

Sesquiterpene product profiles of Cop4, Cop6 and NS1 were analyzed by incubating 20 μL (0.1 mg mL^{-1} in the case of Cop 6 and 0.2 mg mL^{-1} in the case of Cop 4 and NS1) of purified enzyme in 180 μL of terpene synthase buffer containing one of the four prenyl diphosphate substrates investigated (*(E,E)*-FPP, *(Z,E)*-FPP, (±)NPP and *E*-GPP) to yield a final assay concentration of 100 μM. Reaction were carried out in a glass vial for 18 hrs at 25 °C before the headspace of the glass vial was sampled for 10 min by solid phase microextraction (SPME) using a 100 μm polydimethlysiloxane fiber from (Supelco/Sigma-Aldrich Bellefonte, PA). After 10 min absorption, the fiber was inserted into the injection port of a GC/MS for thermal desorption.

To measure the influence of reaction conditions on the product profiles of Cop4 and Cop6 with 100 μM *(E,E)*-FPP as the substrate, the terpene synthase buffer was modified by the addition of NaCl or KCl (final assay concentration: 1 M) or substitution of 10 mM $MgCl_2$ with 10 mM $MnSO_4$. The pH of the reactions was changed by substituting 10 mM Tris-HCl in the terpene synthase buffer with 10 mM of sodium carbonate (pH 10.0) or 10 mM of sodium acetate (pH 5.0) buffer. Reactions were carried out for 18 hrs at 25 °C, 4 °C and 37 °C prior to the analysis of sesquiterpene hydrocarbon products as described above.

Gas chromatography-mass spectrometry (GC/MS) analysis

GC/MS analysis was carried out on a HP GC 7890A coupled to anion-trap mass spectrometer HP MSD triple axis detector (Agilent Technologies, Santa Clara, CA). Separation was carried out using a HP-1MS capillary column (30 m × 0.25 mm inner diameter × 1.0 μm) with an

injection port temperature of 250 °C and helium as a carrier gas. Mass spectra were recorded in electron impact ionization mode. Volatile compounds adsorbed on a fiber from the enzyme reaction headspace were desorbed for 10 min in the injection port. The temperature program started at 60 °C and ramped up 8 °C min^{-1} to a final oven temperature of 250 °C. Mass spectra were scanned in the range of 5–300 atomic mass units at 1 s intervals.

For product identification, the retention index (RI) of each compound peak was determined by calibrating the GC-MS first with a C8-C40 alkane mix. Retention indices and mass spectra of compound peaks were compared to reference data in MassFinder's (software version 3) terpene library [47]. In addition, essential oils with known terpene compositions were used as authentic standards as described in Supplemental Table 1.

Absolute configuration determination

To determine the absolute configuration of several sesquiterpenes described in this study we used chiral GC-MS analysis for comparison of retention times with reference compounds. Sesquiterpenes were separated on a Quiral β-cyclodextrin column (25 m × 0.25mm × 0.125 μm)(Chirasil-Dex, Varian Inc., Palo Alto, CA) using a temperature program that started at 40 °C for 2 min followed by ramping the temperature at 3 °C min^{-1} to a final oven temperature of 200 °C. Mass spectra were scanned in the range of 5–300 atomic mass units at 1 s intervals.

For chiral GC-MS analysis of β-bisabolene, racemic β-bisabolene was kindly provided by Prof. Degenhardt and used as an authentic standard for comparison with Cop4 and Cop6 reaction products (Figure 1). Enantiomers were assigned by comparison with the β-bisabolene present in Bergamot essential oil, which contains only (*6S*)-β-bisabolene (**16s**), as described by Köllner et al. [38]. The absolute configuration of germacrene D (**7s**) synthesized by Cop4 was determined by comparison with germacrene D enantiomers present in the essential oil of *Solidago canadensis*. In this essential oil, the (+) enantiomer is more abundant [72] (Supplemental Figure 4). *Amyris balsamifera* essential oil contains only one enantiomer of cadina-4,11-diene (**14s**) with known absolute configuration [47]. Cadina-4,11-diene (14s) in this essential oil was therefore used as reference compound to determine the absolute configuration of cadina-4,11-diene (**14s**) synthesized by Cop4 with (*Z,E*)-FPP as the substrate (Supplemental Figure 6). Finally, the absolute configuration of the Cop6 reaction product α–cuprenene (**3s**) was indirectly determined via comparison of its oxidation product α-cuparene with a synthetic standard compound containing 98% (+)-α-cuparene and 2% (−)-α-cuparene. Dauben and Oberhänsli [73] report the isolation and synthesis of cuprenenes that under retention of absolute configuration slowly convert into the corresponding, aromatic cuparenes after prolonged air exposure. *In vitro* reactions of Cop6 with (*E,E*)-FPP as a substrate were therefore left standing for up to 30 days at 30 °C with periodic analysis of products formed. Over time, the ring oxidized α-cuparene accumulates (Supplemental Figure 3).

Structural modeling of Cop 4 and Cop 6 sesquiterpenes synthases

Structural models in the open, unliganded conformation were built using the structure of trichodiene synthase from *F. sporotrichoides* [52] (PDB # 1JFA, chain A) for Cop6 (44% amino acid sequence similarity) and of aristolochene synthase from *A. terreus* (PDB #2E40, chain D) [20] for Cop4 (39% amino acid sequence similarity). Crystal structures of trichodiene (PDB# 2Q9z, chain B) [48] and of aristolochene synthase (PDB# 2OA6, chain D) [20] in the closed formation, liganded with Mg^{2+} and pyrophosphate (PPi), were used to built the corresponding models for Cop6 and Cop4. Models were built using the Swiss Model homology-modeling server and using the alignment mode [74]. This method assesses protein structures using three-dimensional profiles. Structures are validated by comparison of an atomic model with its amino acid sequence and assignment of positive (good compatibility) or negative scores for each amino acid position. Models generated in this study have very good

compatibility scores. Protein models were visualized and aligned with their template structure using PyMol 0.99 developed by DeLano Scientific LLC (San Francisco, CA). Active site volumes were calculated with CASTp [75] (using the CASTpyMol version 2.0).

Supplementary Material

Refer to Web version on PubMed Central for supplementary material.

Acknowledgments

This research was supported by the National Institute of Health Grant GM080299 (to CSD). We thank Prof. Jörg Degenhardt from the Max Planck Institute for Chemical Ecology, Jena, Germany, for his gift of the β-bisabolene standard.

References

1. Nobeli I, Favia AD, Thornton JM. Nat Biotechnol 2009;27:157. [PubMed: 19204698]
2. Tokuriki N, Tawfik DS. Science 2009;324:203. [PubMed: 19359577]
3. Christianson DW. Curr Opin Chem Biol 2008;12:141. [PubMed: 18249199]
4. Buckingham, J. Dictionary of natural products (online version). Vol. version 17.1. CHEMnetBASE, Chapman & Hall; 2009.
5. Croteau, R.; Cane, DE. Methods Enzymol. Press, A., editor. Vol. 110. New York: 1985. p. 383
6. Davis EM, Croteau R. Top Curr Chem 2000;209:54.
7. Yoshikuni Y, Martin VJ, Ferrin TE, Keasling JD. Chem Biol 2006;13:91. [PubMed: 16426975]
8. Greenhagen BT, O'Maille PE, Noel JP, Chappell J. Proc Natl Acad Sci U S A 2006;103:9826. [PubMed: 16785438]
9. O'Maille PE, Malone A, Dellas N, Andes Hess B Jr, Smentek L, Sheehan I, Greenhagen BT, Chappell J, Manning G, Noel JP. Nat Chem Biol 2008;4:617. [PubMed: 18776889]
10. Lesburg CA, Caruthers JM, Paschall CM, Christianson DW. Curr Opin Struct Biol 1998;8:695. [PubMed: 9914250]
11. Cane DE, Kang I. Arch Biochem Biophys 2000;376:354. [PubMed: 10775423]
12. Christianson DW. Chem Rev 2006;106:3412. [PubMed: 16895335]
13. Vedula LS, Jiang J, Zakharian T, Cane DE, Christianson DW. Arch Biochem Biophys 2008;469:184. [PubMed: 17996718]
14. Lee S, Chappell J. Plant Physiol 2008;147:1017. [PubMed: 18467455]
15. Steele CL, Crock J, Bohlmann J, Croteau R. J Biol Chem 1998;273:2078. [PubMed: 9442047]
16. Cane DE, Sohng JK, Lamberson CR, Rudnicki SM, Wu Z, Lloyd MD, Oliver JS, Hubbard BR. Biochemistry 1994;33:5846. [PubMed: 8180213]
17. Back K, Chappell J. J Biol Chem 1995;270:7375. [PubMed: 7706281]
18. Starks CM, Back KW, Chappell J, Noel JP. Science 1997;277:1815. [PubMed: 9295271]
19. Caruthers JM, Kang I, Rynkiewicz MJ, Cane DE, Christianson DW. J Biol Chem 2000;275:25533. [PubMed: 10825154]
20. Shishova EY, Di Costanzo L, Cane DE, Christianson DW. Biochemistry 2007;46:1941. [PubMed: 17261032]
21. Cane DE, Pawlak JL, Horak RM. Biochemistry 1990;29:5476. [PubMed: 2386780]
22. Hohn TM, Beremand PD. Gene 1989;79:131. [PubMed: 2777086]
23. Gennadios HA, Gonzalez V, Di Costanzo L, Li A, Yu F, Miller DJ, Allemann RK, Christianson DW. Biochemistry 2009;48:6175. [PubMed: 19489610]
24. Agger S, Lopez-Gallego F, Schmidt-Dannert C. Mol Microbiol 2009;72:1181. [PubMed: 19400802]
25. Agger S, Lopez-Gallego F, Schmidt-Dannert C. Mol Microbiol 2009;72:1307.
26. Bu'Lock JD, Darbyshire J. Phytochemistry 1976;15:2004.

27. Agger SA, Lopez-Gallego F, Hoye TR, Schmidt-Dannert C. J Bacteriol 2008;190:6084. [PubMed: 18658271]
28. Alchanati I, Patel JAA, Liu JG, Benedict CR, Stipanovic RD, Bell AA, Cui YX, Magill CW. Phytochemistry 1998;47:961.
29. Kim SH, Heo K, Chang YJ, Park SH, Rhee SK, Kim SU. J Nat Prod 2006;69:758. [PubMed: 16724836]
30. Picaud S, Mercke P, He X, Sterner O, Brodelius M, Cane DE, Brodelius PE. Arch Biochem Biophys 2006;448:150. [PubMed: 16143293]
31. Schenk DJ, Starks CM, Manna KR, Chappell J, Noel JP, Coates RM. Arch Biochem Biophys 2006;448:31. [PubMed: 16309622]
32. Benedict CR, Lu JL, Pettigrew DW, Liu JG, Stipanovic RD, Williams HJ. Plant Physiol 2001;125:1754. [PubMed: 11299356]
33. Cane DE, Yang G, Xue Q, Shim JH. Biochemistry 1995;34:2471. [PubMed: 7873526]
34. Vedula LS, Cane DE, Christianson DW. Biochemistry 2005;44:12719. [PubMed: 16171386]
35. Vedula LS, Rynkiewicz MJ, Pyun HJ, Coates RM, Cane DE, Christianson DW. Biochemistry 2005;44:6153. [PubMed: 15835903]
36. Kollner TG, Gershenzon J, Degenhardt J. Phytochemistry 2009;70:1139. [PubMed: 19646721]
37. Kollner TG, O'Maille PE, Gatto N, Boland W, Gershenzon J, Degenhardt J. Arch Biochem Biophys 2006;448:83. [PubMed: 16297849]
38. Kollner TG, Schnee C, Li S, Svatos A, Schneider B, Gershenzon J, Degenhardt J. J Biol Chem 2008;283:20779. [PubMed: 18524777]
39. Bohlmann J, Crock J, Jetter R, Croteau R. Proc Natl Acad Sci U S A 1998;95:6756. [PubMed: 9618485]
40. Kollner TG, Schnee C, Gershenzon J, Degenhardt J. Plant Cell 2004;16:1115. [PubMed: 15075399]
41. Mercke P, Crock J, Croteau R, Brodelius PE. Arch Biochem Biophys 1999;369:213. [PubMed: 10486140]
42. Cane DE, Ha HJ. J Am Chem Soc 1988;110:6865.
43. Lin X, Cane DE. J Am Chem Soc 2009;131:6332. [PubMed: 19385616]
44. Cane DE, Xue Q. J Am Chem Soc 1996;118:1563.
45. Adio AM, Paul C, Kloth P, Konig WA. Phytochemistry 2004;65:199. [PubMed: 14732279]
46. Nabeta K, Fujita M, Komuro K, Katayama K, Takasawa T. J Chem Soc; Perkin Trans 1 1997:2065.
47. Konig WA, Bulow N, Saritas Y. Flavour Fragr J 1999;14:367.
48. Vedula LS, Zhao YX, Coates RM, Koyama T, Cane DE, Christianson DW. Arch Biochem Biophys 2007;466:260. [PubMed: 17678871]
49. Croteau R, Satterwhite DM. J Biol Chem 1989;264:15309. [PubMed: 2768265]
50. Schwab W, Williams DC, Davis EM, Croteau R. Arch Biochem Biophys 2001;392:123. [PubMed: 11469803]
51. Crock J, Wildung M, Croteau R. Proc Natl Acad Sci U S A 1997;94:12833. [PubMed: 9371761]
52. Rynkiewicz MJ, Cane DE, Christianson DW. Proc Natl Acad Sci U S A 2001;98:13543. [PubMed: 11698643]
53. Rynkiewicz MJ, Cane DE, Christianson DW. Biochemistry 2002;41:1732. [PubMed: 11827517]
54. He X, Cane DE. J Am Chem Soc 2004;126:2678. [PubMed: 14995166]
55. Schmidt CO, Bouwmeester HJ, Bulow N, Konig WA. Arch Biochem Biophys 1999;364:167. [PubMed: 10190971]
56. Schmidt CO, Bouwmeester HJ, de Kraker JW, Konig WA. Angew Chem, Intl Ed 1998;37:1400.
57. Felicetti B, Cane DE. J Am Chem Soc 2004;126:7212. [PubMed: 15186158]
58. Cane DE, Xue Q, VanEpp JE. J Am Chem Soc 1996;118:8499.
59. Mercke P, Bengtsson M, Bouwmeester HJ, Posthumus MA, Brodelius PE. Arch Biochem Biophys 2000;381:173. [PubMed: 11032404]
60. Tholl D, Chen F, Petri J, Gershenzon J, Pichersky E. Plant J 2005;42:757. [PubMed: 15918888]
61. Croteau R, Satterwhite DM, Cane DE, Chang CC. J Biol Chem 1988;263:10063. [PubMed: 3392006]

62. Gambliel H, Croteau R. J Biol Chem 1982;257:2335. [PubMed: 7037765]
63. Zahn TJ, Eilers M, Guo ZM, Ksebati MB, Simon M, Scholten JD, Smith SO, Gibbs RA. J Am Chem Soc 2000;122:7153.
64. Shishova EY, Yu F, Miller DJ, Faraldos JA, Zhao Y, Coates RM, Allemann RK, Cane DE, Christianson DW. J Biol Chem 2008;283:15431. [PubMed: 18385128]
65. Hyatt DC, Youn B, Zhao Y, Santhamma B, Coates RM, Croteau RB, Kang C. Proc Natl Acad Sci U S A 2007;104:5360. [PubMed: 17372193]
66. Landmann C, Fink B, Festner M, Dregus M, Engel KH, Schwab W. Arch Biochem Biophys 2007;465:417. [PubMed: 17662687]
67. Picaud S, Olofsson L, Brodelius M, Brodelius PE. Arch Biochem Biophys 2005;436:215. [PubMed: 15797234]
68. Picaud S, Brodelius M, Brodelius PE. Phytochemistry 2005;66:961. [PubMed: 15896363]
69. Shao Y, Eummer JT, Gibbs RA. Org Lett 1999;1:627. [PubMed: 10823190]
70. Popják G, Schroepfer G, Cornforth JW. Biochem Biophys Res Commun 1961;6:438.
71. Jez JM, Ferrer JL, Bowman ME, Dixon RA, Noel JP. Biochemistry 2000;39:890. [PubMed: 10653632]
72. Schmidt CO, Bouwmeester HJ, de Kraker J-W, König WA. Angewandte Chemie International Edition 1998;37:1400.
73. Dauben WG, Oberhansli P. J Org Chem 1966;31:315.
74. Bordoli L, Kiefer F, Arnold K, Benkert P, Battey J, Schwede T. Nat Protoc 2009;4:1. [PubMed: 19131951]
75. Dundas J, Ouyang Z, Tseng J, Binkowski A, Turpaz Y, Liang J. Nucleic Acids Res 2006;34:W116. [PubMed: 16844972]
76. de Kraker JW, Franssen MCR, de Groot A, Konig WA, Bouwmeester HJ. Plant Physiol 1998;117:1381. [PubMed: 9701594]

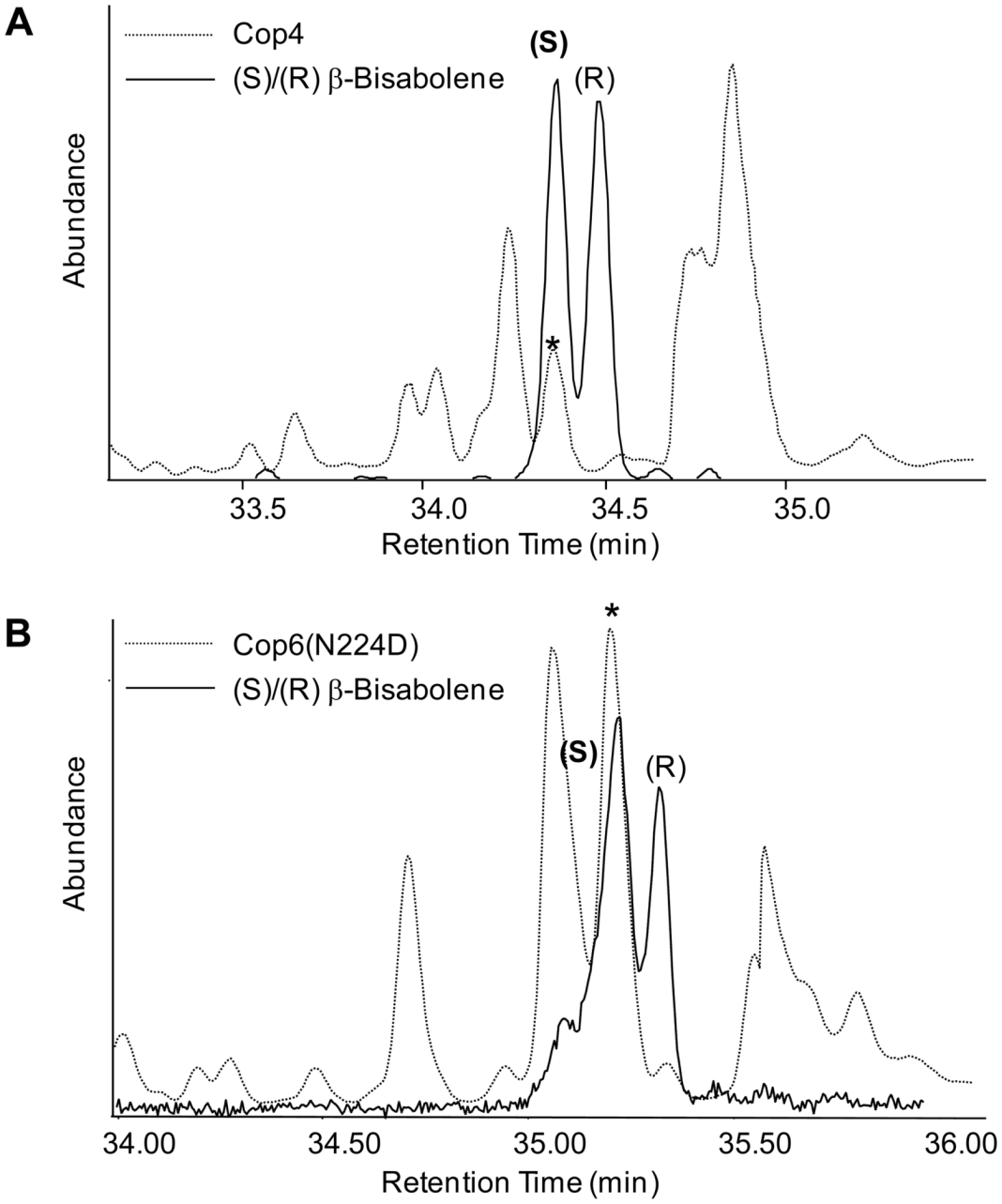

Figure 1. Stereochemical analysis of β-bisabolene products synthesized from *(Z,E)*-FPP

Reaction products of purified Cop4 (A) and mutant Cop6 N224D (B) with *(Z,E)*-FPP were separated by chiral GC-MS (dotted trace) and identified using authentic β–bisabolene standards (solid trace). Peaks labeled with an asterisk correspond to the Cop4 and Cop6 β-bisabolene reaction products.

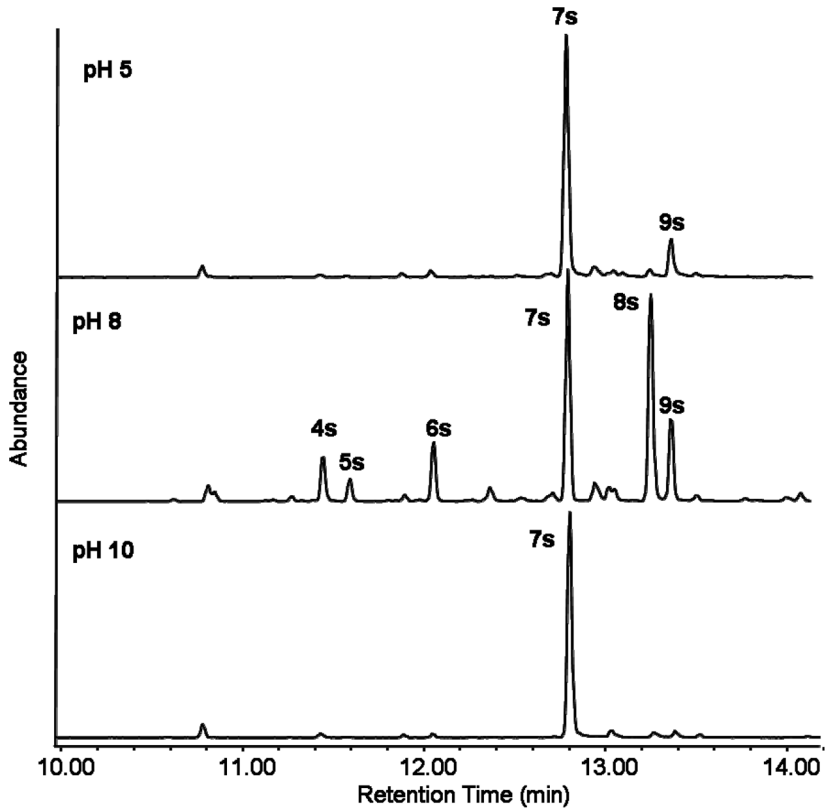

Figure 2. Effect of pH on the product selectivity of Cop4 with *(E,E)*-FPP

Reactions of purified Cop4 with *(E,E)*-FPP were carried under different pH conditions. Reaction products were separated by GC-MS and compound peaks identified by comparison of mass spectra and RI values with those in reference libraries and with authentic standards.

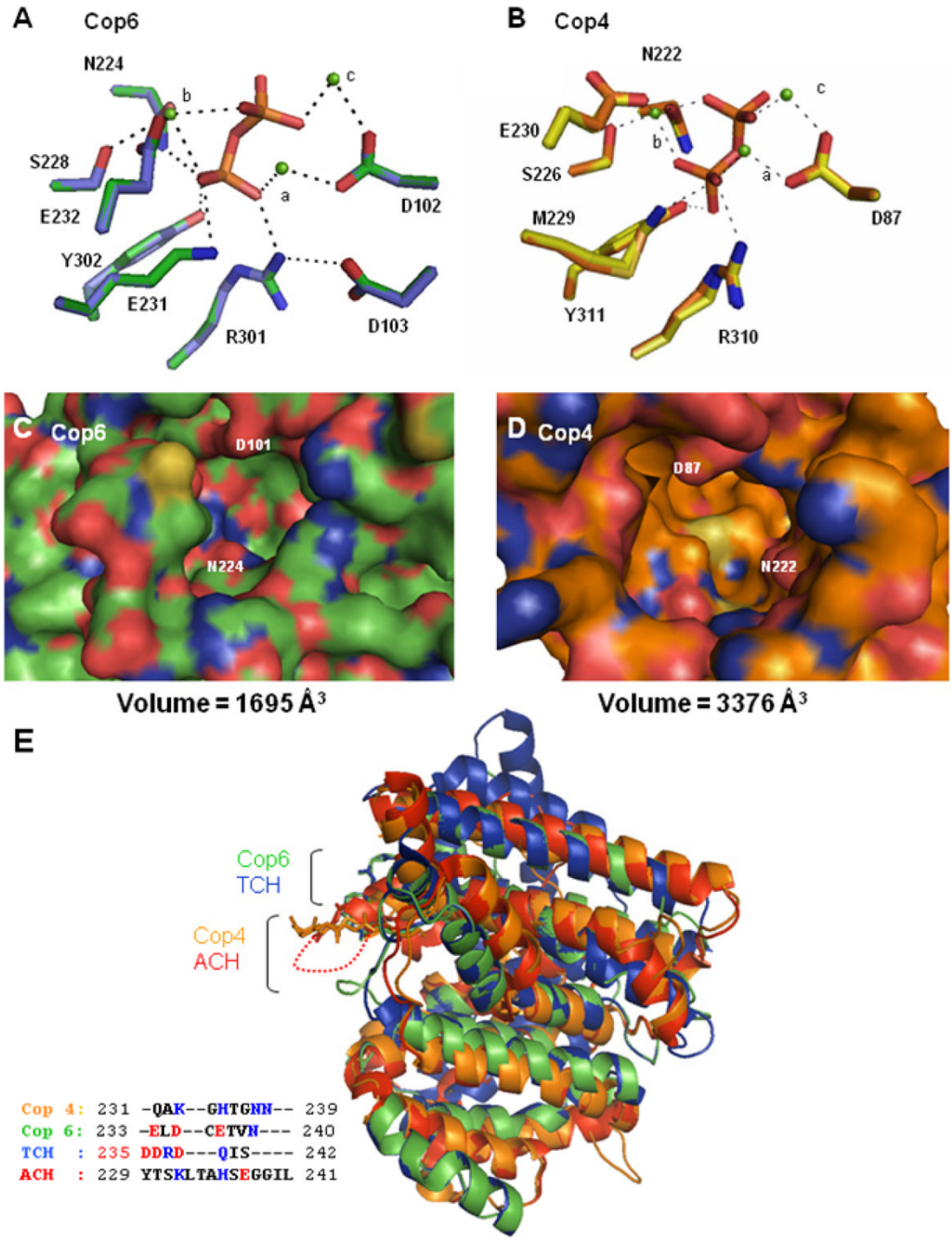

Figure 3. Structural modeling of Cop4 and Cop6 based on the structures of aristolochene synthase (ACH) [20] and trichodiene synthase (TCH) [48], respectively

Top panels: Hydrogen bond and metal coordination interactions in the enzyme-Mg2+-PPi-complex for the Cop6 (A) (green side chains) and Cop4 (B) (orange side chains) models. Depicted side chains of the conserved DDXXD/E, NSE/DTE and basic motif (XRY) are superimposed with corresponding side chains from their respective template structures (TCH, purple; ACH, yellow). Mg2+ ions are shown in green and complexed PPi is located in the center of the networks. Center panels: View into the active site cavities of unliganded Cop6 (C) (green alpha carbons) and Cop4 (D) (orange alpha carbons). Positively charged and negatively charged amino acid residues are shown in blue and red respectively. Bottom panel:

Superimposition of the unliganded Cop4 and Cop6 models with the unliganded structures of THC and ACH (E). Loops covering the active sites of the enzymes are labeled and colors correspond to those of their alpha carbon backbones in the superimposition. Inset shows the amino acid residues of the different loops. Basic (blue) and acidic (red) amino acid residues are highlighted.

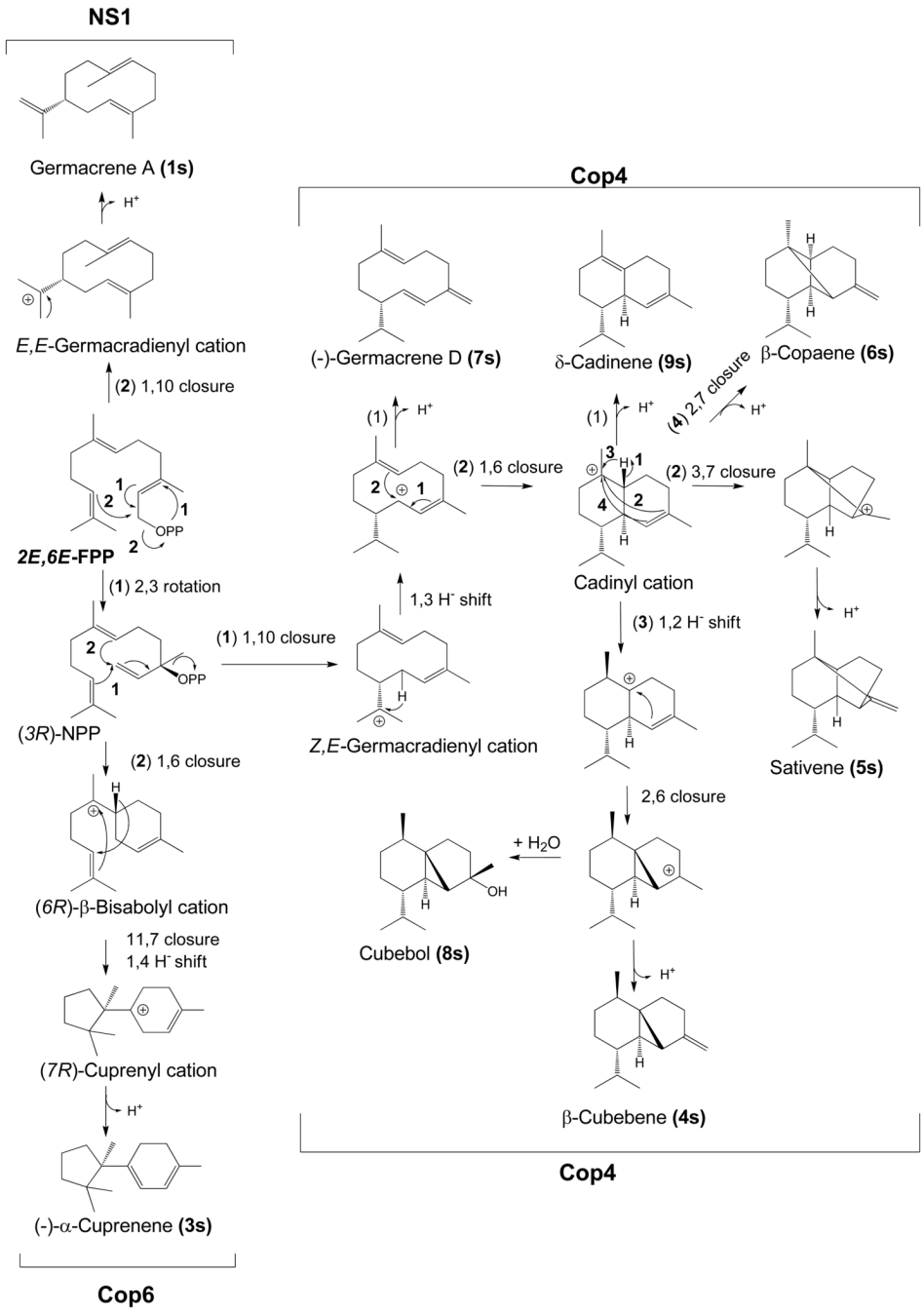

Scheme 1. Proposed reaction mechanism accounting for the identified products generated from *(E,E)*-FPP by Cop4, Cop6 and NS1

Numbered reaction arrows indicate different branch points in the cyclization reaction. Relative amounts of products formed by each enzyme are shown in Table 2.

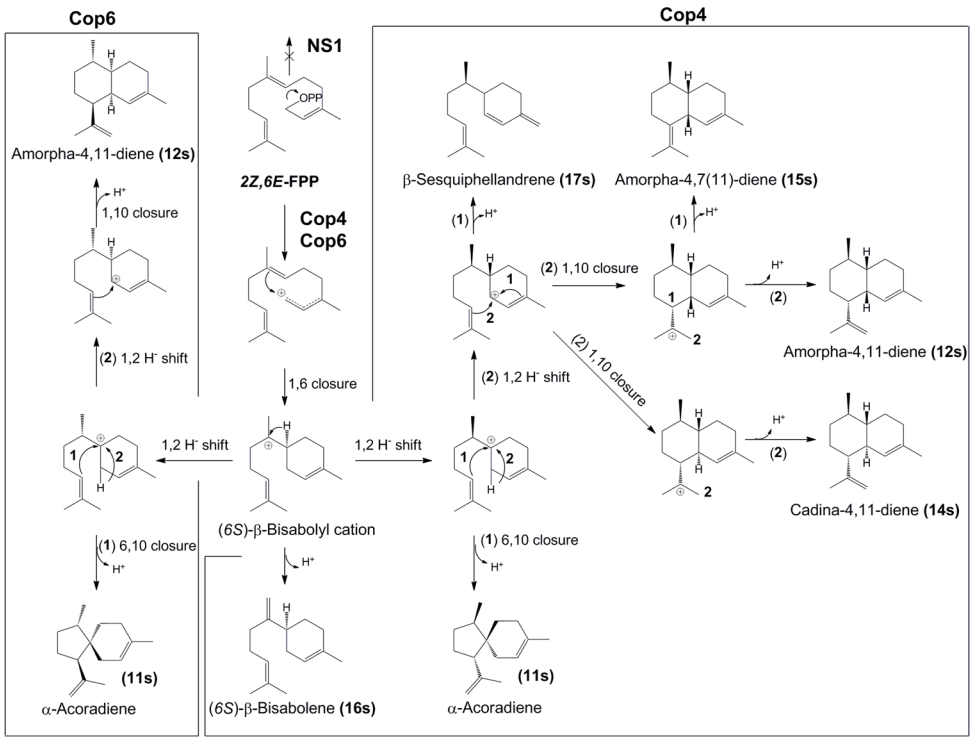

Scheme 2. Proposed reaction mechanism accounting for the identified products generated from *(Z,E)*-FPP by Cop4, Cop6 and NS1

Numbered reaction arrows indicate different branch points in the cyclization reaction. Relative amounts of products formed by each enzyme are shown in Table 2. (6S)-β-bisabolene is also formed as a product (18%) by the mutant form of Cop 6 (N224D), thus providing strong evidence for the common 6S stereochemistry of β-bisabolyl cation intermediate generated by Cop 6.

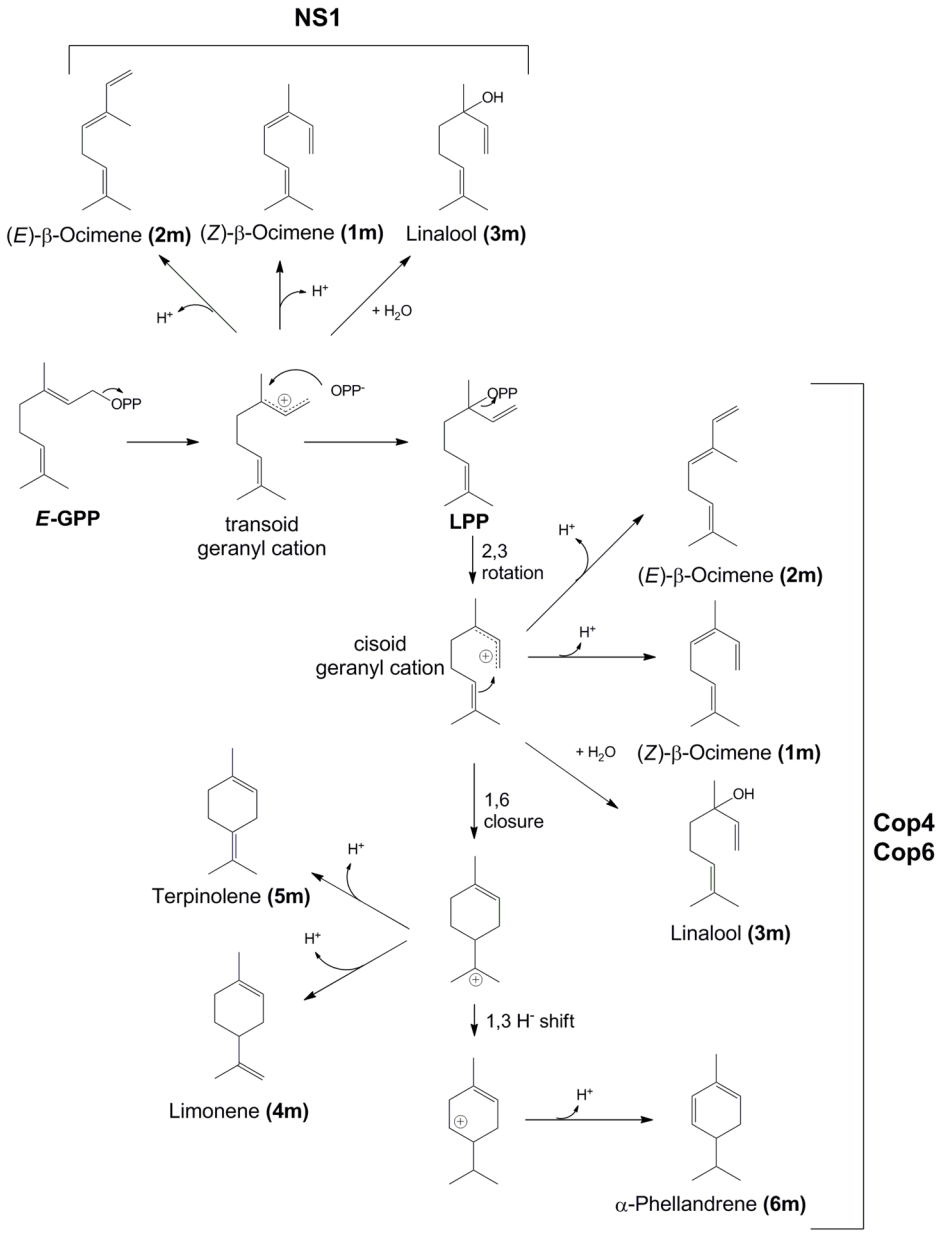

Scheme 3. Postulated mechanism of monoterpene formation from *E*-GPP

Acylic monoterpenes produced by NS1 are proposed to be derived from a transoid geranyl cation, while the acyclic and cyclic monoterpene products of Cop4 and Cop6 are postulated to involve the generation of a cisoid geranyl cation (neryl cation). Relative amounts of products formed by each enzyme are shown in Table 2.

Table 1

Kinetic constants of Cop4 and Cop6 with *(E,E)*-, *(Z,E)*-FPP and *E*-GPP

	K_m (μM)			k_{cat} (s^{-1})			k_{cat}/K_m (s^{-1} M^{-1})(×10^3)		
	***(E,E)*-FPP**	***(Z,E)*-FPP**	***E*-GPP**	***(E,E)*-FPP**	***(Z,E)*-FPP**	***E*-GPP**	***(E,E)*-FPP**	***(Z,E)*-FPP**	***E*-GPP**
NS1	3.8±0.5	na *[a]*	1.4±0.5	(5.3±0.1)×10^{-2}	na *[a]*	(20±1)×10^{-4}	14	na *a)*	1.35
Cop6	7.6±2.4	nd *[b]*	1.5±0.6	(67±0.7)×10^{-2}	nd *[b]*	(3.5±0.3)×10^{-2}	88	nd *b)*	24
Cop4	11±3	20±2	24±8	(1.2±0.1)×10^{-2}	(0.25±0.04)×10^{-2}	(1.6±0.3)×10^{-4}	1	0.22	0.007

Kinetic constants are compared to those obtained with the bacterial germacrene A synthase NS1 that uses the all-trans pathway of catalysis.

*[a]*na: No activity detected.

*[b]*nd: Activity too low for kinetic measurements.

Table 2

Terpenoid product profiles of purified Cop4 and Cop6 with *(E,E)*-, *(Z,E)*-FPP and *E*-GPP

Product (%) [a]		1s[b]	2s[b]	3s	4s	5s	6s	7s	8s	9s	10s	11s	12s	13s	14s	15s	16s	17s	ND[c]
		1m	2m	3m	4m	5m	6m												
NS1	*(E,E)*-FPP	93.5	6.5	-	-	-	-	-	-	-	-	-	-	-	-	-	-	-	-
	(Z,E)-FPP	-	-	-	-	-	-	-	-	-	-	-	-	-	-	-	-	-	-
	E-GPP	25	9	66	-	-	-												-
Cop6	*(E,E)*-FPP	-	-	98.2	-	-	-	-	-	-	-	-	-	-	-	-	-	-	1.8
	(Z,E)-FPP	-	-	-	-	-	-	-	-	-	45	5.2	25.6	16.3	-	-	-	-	7.9
	E-GPP	9.2	7.11	34.6	45	4	-												-
Cop4	*(E,E)*-FPP	-	-	-	5.7	2.8	7.4	29.3	28.2	10.4	-	-	-	-	-	-	-	-	16.1
	(Z,E)-FPP	-	-	-	-	-	-	-	-	-	-	27.7	10	-	13.3	6.4	4.2	15	23.7
	E-GPP	61	9.1	-	23.7	2.5	3.6												9.3

Product profiles are compared to those obtained with the bacterial germacrene A synthase NS1 that uses the all-trans pathway of catalysis. Sesquiterpene products obtained with *(E,E)* or *(Z,E)*-FPP have compound numbers ending with an "s", while monoterpene products obtained with *E*-GPP (shaded cells) have compound numbers ending with an "m". Structures corresponding to shown compound numbers are found in Schemes 1 and 2 (sesquiterpenes), and Scheme 3 (monoterpenes). Underlined compounds represent major sesquiterpene products that could not be identified.

[a] Percentages are averages calculated from product profiles of three independent *in vitro* reactions. The error was less than 5% in all cases. See Supplemental Figure 1 and 2 (sesquiterpenes) and Supplemental Figure 7 and 8 (monoterpenes) for representative GC/MS chromatograms of product profiles.

[b] 1s and 2s are the heat induced Cope rearrangement products of germacrene A: β-elemene (1s) and *cis*-β-elemene (2s) [76]

[c] ND: Sum of minor products that could not be identified.

Table 3

Sesquiterpene product profile of purified Cop4 with *(E,E)*-FPP under different reaction conditions

Conditions				Products (%)[a]						
pH	**NaCl (M)**	**T (°)C**	**Cation (10 mM)**	**4s**	**5s**	**6s**	**7s**	**8s**	**9s**	**ND[b]**
10.0	**0**	**25**	**Mg^{2+}**	-	-	-	91.1	-	-	8.9
5.0	**0**	**25**	**Mg^{2+}**	-	-	-	84.3	-	12.32	3.3
8.0	**0**	**25**	**Mg^{2+}**	5.7	2.8	7.4	29.3	28.2	10.4	16.1
8.0	**0**	**4**	**Mg^{2+}**	5.9	2.3	6.2	37.8	27.2	11.7	8.9
8.0	**0**	**37**	**Mg^{2+}**	7.1	5.3	12.3	22.3	22.3	13.3	17.3
8.0	**1**	**25**	**Mg^{2+}**	4.8	1.5	4.2	17.7	33.5	10.2	28.0
8.0	**0**	**25**	**Mn^{2+}**	5.5	-	2.3	48.7	20.2	7.1	16.2
8.0	**0**	**25**	**K^{+}**	10.7	3.7	10.3	19.4	34.2	15	11.3

Structures corresponding to compound numbers shown are found in Scheme 1.

[a] Percentages are averages calculated from product profiles of three independent *in vitro* reactions. The error was less than 5% in all cases.

[b] ND: Sum of minor products that could not be identified.